Paper 45

The Use of Geophysics in the Ring of Fire, James Bay Lowlands – The Chromite Story

Rainsford, D.R.B. [1], Diorio, P.A. [2], Hogg, R.L.S. [3], Metsaranta, R.T. [1]

1. Ontario Geological Survey, Sudbury, ON, Canada
2. GeophysicsOne Inc., Oakville, ON, Canada
3. Scott Hogg & Associates, Toronto, ON, Canada

ABSTRACT

In less than a decade the "Ring of Fire" (RoF), an area of Archean supracrustal and mafic to ultramafic intrusive rocks in the James Bay lowlands that is partially covered by Paleozoic sediments and almost completely blanketed by glacial drift, has been transformed from virgin territory to a potentially world-class polymetallic mining camp awaiting development. This paper concentrates on the chromite discoveries and the geophysical methods used to detect and define the deposits. Although the initial indication of chromite was serendipitous, the recognition of the significance of the discovery and the realignment of geophysical programs to take advantage of the characteristics of the mineralization and associated host rocks led to the rapid discovery of six chromite ore bodies. Physical rock property data indicate why gravity, magnetic and electromagnetic (EM) methods were effective in exploring for this type of deposit. Typical ground and airborne responses are presented and discussed. Airborne gravity gradiometry was able to define mafic and ultramafic rock units, including the host rocks of the chromite mineralization, but had insufficient resolution to detect the deposits themselves. In a region almost devoid of outcrop, airborne gravity was able to improve geological understanding by distinguishing between magnetic granitoid rocks and mafic/ultramafic rocks with similar magnetic responses. 3-D inversion of airborne magnetic and gravity data creates voluminous voxel data sets which are hard to visualize conventionally. Multi-parameter classification of the 3-D models, combined with knowledge of physical rock properties, demonstrates how rock units may be predicted and delineated. Four of the six deposits, discovered so far, are near-surface and amenable to direct geophysical detection. As exploration in the vicinity of known deposits in the RoF matures, work will likely focus on deeper deposits and geophysics will be required to define favourable stratigraphy which, along with tighter integration of deposit models, structural geological controls and lithogeochemistry, could be used to locate otherwise blind targets. However, at a regional scale, additional ultramafic intrusions with chromite potential remain to be explored via the conventional ground geophysical methods that appear to be required to effectively target mineralization. While the emphasis of this paper has been the chromite discoveries, the short history of the RoF has shown that explorationists need to be open to the unexpected and be prepared to take advantage when the opportunity arises.

REGIONAL GEOLOGY

The geology of the "Ring of Fire" (RoF) region comprises a variety of Precambrian rocks, flat-lying Paleozoic carbonate-dominated strata and unconsolidated Quaternary deposits. The poorly exposed Precambrian geology includes Mesoarchean to Neoarchean supracrustal rocks of the McFaulds Lake greenstone belt (MLGB) and a variety of intrusive rocks of felsic to ultramafic in composition as well as Proterozoic dike swarms (Matachewan, Marathon, Pickle Crow and Mackenzie swarms) and Mesoproterozoic kimberlite intrusions (Kyle field) (Figure 1, Sage, 2000; Stott and Josey, 2009; Metsaranta and Houlé, 2017a, 2017b, 2017c;).

Paleozoic strata unconformably overlie Precambrian rocks across the eastern portions of the region and an oxidized to reduced (depending on depth beneath the unconformity) weathering and/or alteration profile affects the Precambrian basement to a variable depth (0 to 10's of metres) beneath the unconformity. The Paleozoic rocks form a generally east and northeastward thickening wedge representing lithostratigraphic units of Ordovician to Silurian age (see Armstrong, 2011; Ratcliffe and Armstrong, 2013). Quaternary and recent sediments cover the bulk of the area apart from sparse bedrock exposures.

The MLGB is an arcuate (>200 km long) greenstone belt that records episodic volcanism, sedimentation and tectonism spanning from ca. 2.83 Ga to 2.70 Ga. It has been subdivided into seven tectonostratigraphic assemblages including two Mesoarchean volcanic-dominated assemblages (Butler - ca. 2828 Ma / Attawapiskat - ca. 2811 Ma); four Neoarchean volcanic-dominated assemblages (Victory - ca. 2797–2781 Ma / Winiskisis- ca. 2757 Ma / Muketei - ca. 2735 Ma / Kitchie - in part <2725 Ma); and one sedimentary-dominated assemblage (Tappan - <2702 Ma) (Metsaranta et al., 2015).

In "Proceedings of Exploration 17: Sixth Decennial International Conference on Mineral Exploration" edited by V. Tschirhart and M.D. Thomas, 2017, p. 649–662

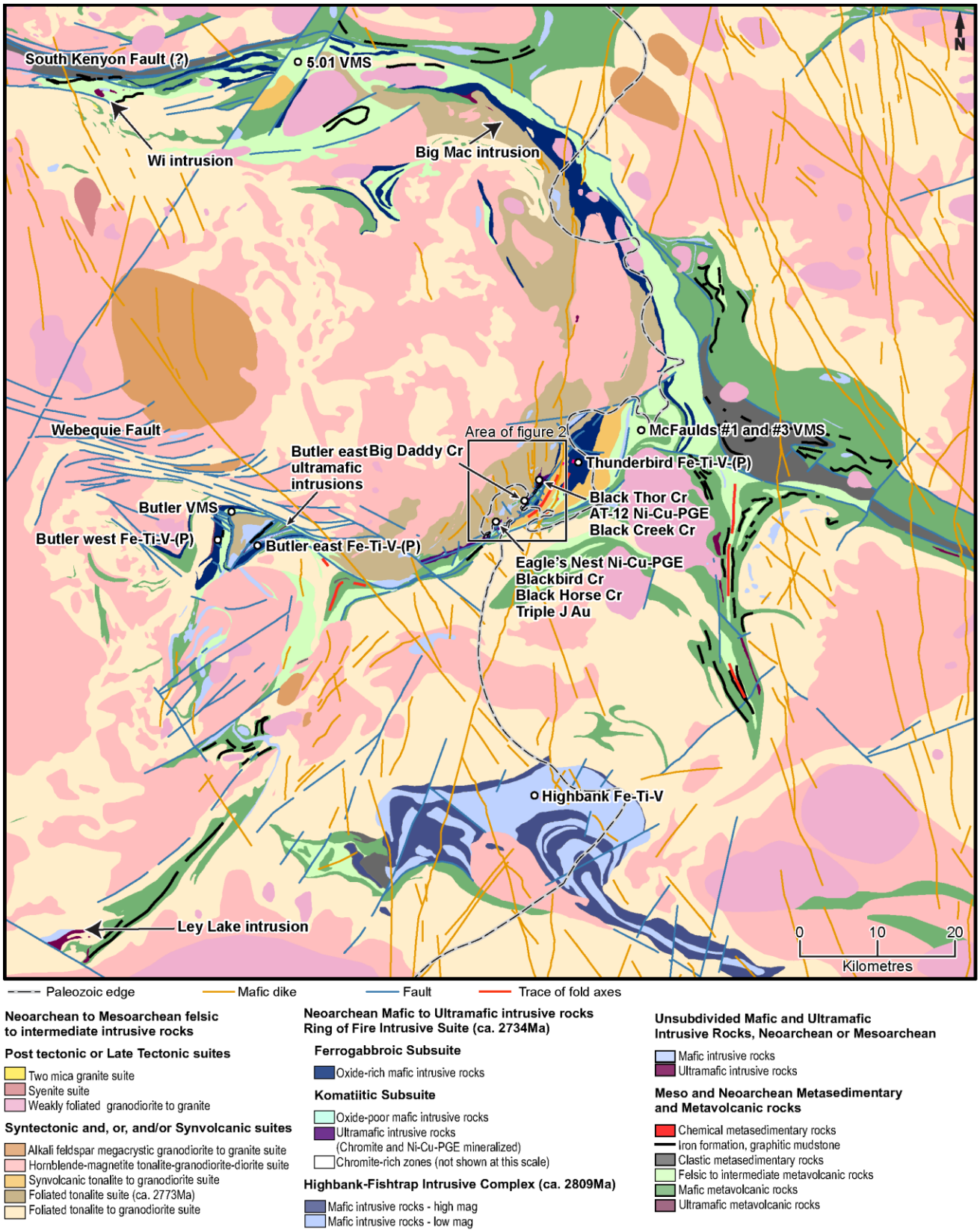

Figure 1: Simplified geology of the RoF area. Modified from Metsaranta and Houlé (2017a, b, c).

Felsic to intermediate intrusive rocks in the RoF region form large composite, greenstone belt-bounding batholiths as well as discrete plutons. Early tonalite-dominated suites range in ages from ca. 2804 Ma to 2773 Ma and may be coeval with the older supracrustal assemblages (Metsaranta and Houlé, 2017a, b, c). Another suite of synvolcanic granodioritic-tonalitic plutons intruded the MLGB in the central part of the RoF region at ~2734 Ma (Metsaranta and Houlé, 2017a, b, c). Granodioritic to tonalitic plutons emplaced at ca. 2728–2710 Ma are interpreted to be syntectonic, whereas weakly deformed granodioritic to syenitic plutons, ca. 2704-2661 Ma, are interpreted to be late to post-tectonic (Metsaranta and Houlé, 2017a, b, c).

Mafic-ultramafic intrusions in the RoF region host the bulk of known mineral deposits. Two main subdivisions are identified.
A large, deformed, mafic-dominated, layered intrusive complex, the Highbank Lake intrusive complex (HBLIC) occurs in the southern portion of the region and was emplaced ca. 2809 Ma (Metsaranta and Houlé, 2017c). The HBLIC does not host any known mineral deposits. However, it does contain some anomalous PGE and Fe-Ti-V mineralization.

A Cr-(PGE), Ni-Cu-PGE, and Fe-Ti-V mineralized intrusive suite, generally subconcordant with the MLGB, termed the Ring of Fire intrusive suite (RoFIS) was emplaced at ca. 2734 Ma (e.g. Mungall et al. 2010, Metsaranta and Houlé, 2017b) . The RoFIS includes volumetrically dominant, spatially widespread, ferrogabbroic intrusions and more spatially restricted, ultramafic-dominated intrusions. Syn-RoFIS volcanism, felsic intrusions and ferrogabbroic intrusions (e.g. Thunderbird, Big Mac, Butler) are exposed over much of the MLGB. Additional ultramafic intrusions (e.g. Wi intrusion, Butler area intrusions, Big Mac intrusion, Ley Lake intrusion, Figure 1) are known in the MLGB, but have not been extensively explored. The relationship between the chromite mineralized ultramafic intrusions and ferrogabbroic intrusions is unclear and they may represent: related fractional crystallization products or separate, though time correlative products of mantle melting.

Known chromite mineralized intrusions have been delineated by diamond drilling over a strike length of approximately 13 km and achieve a maximum mapped width of about 3 km based on current drilling constraints (regionally mafic and ultramafic intrusions are more extensive, but are not known to contain chromite deposits). They appear to form northeast striking, sill-like, broadly tabular features, with localized "funnel" shaped apophyses towards the north-northwest. The mineralized intrusions are steeply dipping and appear to form, at a local scale, a homoclinal panel, or broad fold limb that faces towards the southeast stratigraphically (Figure 2). At the Double Eagle intrusive complex (DEIC); (Houlé et al., 2017), located at the southwest end of the known mineralized portion of the intrusion (Figure 2), faults complicate the local stratigraphy. Here, both the lower and upper contacts of the intrusion are shear zones and faults, broadly perpendicular to strike of the intrusions, also offset rock units. At the northeast end of the known mineralized system (Figure 2) i.e. the Black Thor intrusive complex (BTIC); (Houlé et al., 2017) a more complete stratigraphy appears to be preserved despite zones of high strain, which appear to occur dominantly near the boundary between the lower ultramafic portions of the intrusion and the upper mafic-dominated portion of the intrusion. At the DEIC the shear zone at the upper contact of the ultramafic intrusion may have juxtaposed older metavolcanic strata (Metsaranta et al. 2015). Whereas, at the BTIC, overlying rocks may represent syn-intrusion volcanism or older metavolcanic country rocks. Carson et al. (2015) have defined an internal stratigraphy of the BTIC (Figure 3) that serves as an idealized section for the chromite mineralized sills in the area.

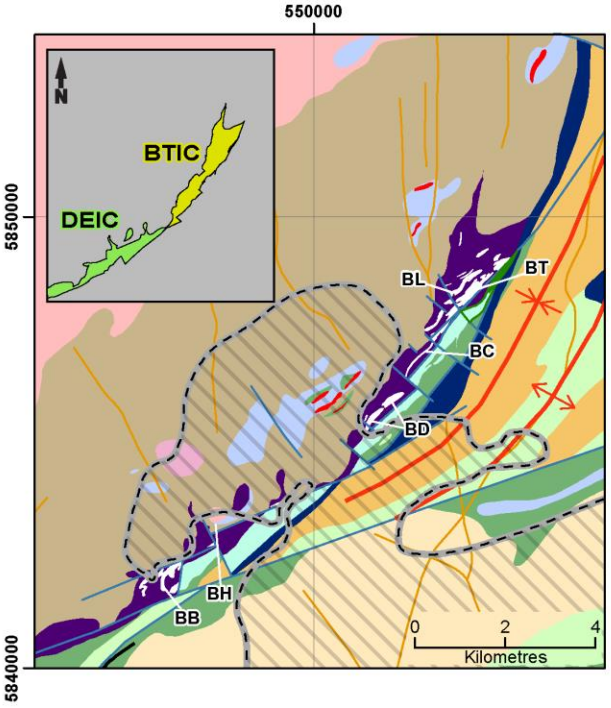

Figure 2: Simplified geology of the central RoF area showing the locations of main chromite deposits and their geological setting. Modified from Metsaranta and Houlé (2017b), Houlé et al. (2017). Legend is the same as Figure 1. Abbreviations: BL=Black Label, BT=Black Thor, BC=Black Creek, BD=Big Daddy, BH=Black Horse, BB=Blackbird. The grey hatch pattern indicates areas inferred to be covered by Paleozoic rocks.

In a simplified sense the stratigraphy in the vicinity of chromite deposits includes:

1. a basement foliated biotite tonalite unit (ca. 2773 Ma) that appears to have intruded an older mafic metavolcanic succession with intercalated magnetite-chert iron formation and relatively homogeneous gabbro
2. possible ultramafic "feeder" dikes hosting the Eagle's Nest Ni-Cu-PGE deposit (DEIC) and AT-12 prospect (BTIC)
3. layered ultramafic sills hosting the stratiform chromite mineralization
4. an upper gabbro unit, likely comagmatic and in gradational contact with chromite mineralized ultramafic rocks
5. a complex stratigraphic hanging wall of mafic metavolcanic rocks of unknown age, RoFIS ferrogabbroic intrusions, felsic intrusions and VMS mineralized bimodal mafic-felsic metavolcanic rocks

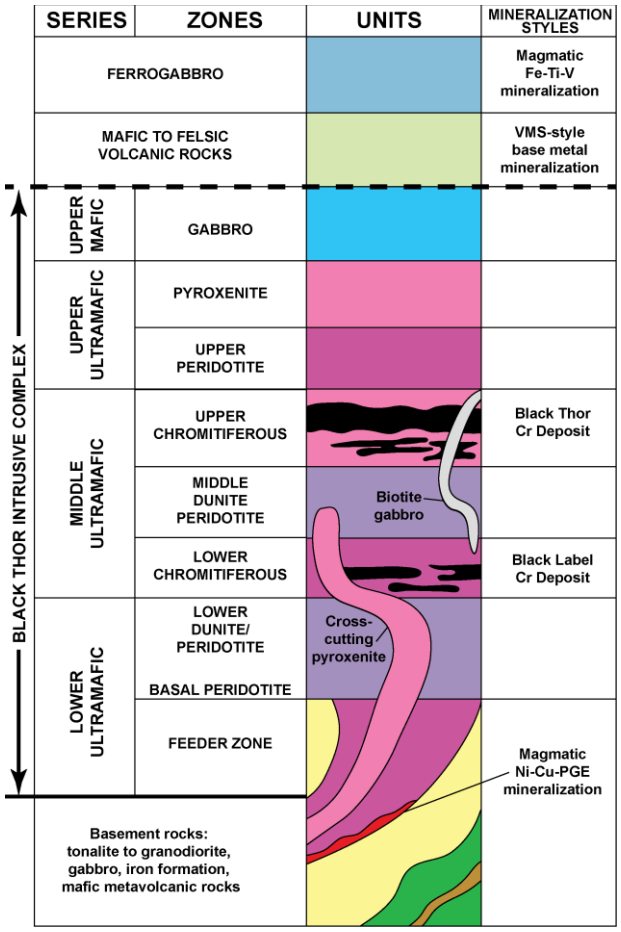

Figure 3: Idealized stratigraphy of the Black Thor intrusive complex and its chromite deposits. Modified from Carson et al. (2015).

CHROMITE DISCOVERIES

As has been described elsewhere (Witherly and Diorio, 2014, Hogg and Munro, 2017), the initial exploration interest in this region was for diamonds which resulted in the discovery of the Victor kimberlite cluster and volcanogenic massive sulphides (VMS) at McFaulds Lake and elsewhere. Subsequent VMS exploration led to the initial discovery of chromite, Ni-Cu-PGE and Fe-Ti-V mineralization in the RoF.

The first indications of chromite mineralization in the RoF region were narrow intersections recognized by geologist Howard Lahti in core from a hole drilled in 2006 by Freewest Resources Inc. Although the hole (FW-06-03) was drilled to test a ground EM anomaly, "*the core did not intersect any sulphides or any other obvious conductor*" (Gowans and Murahwi, 2009) but did yield two, approximately one metre, bands of 23% Cr_2O_3 in serpentinized ultramafic rock. This hole led to the discovery of the Big Daddy chromite deposit. Subsequently, the Eagle's Nest (originally called Eagle One) magmatic sulphide deposit and Eagle Two sulphide mineral occurrence were intersected in 2007 and 2008 respectively by Noront Resources Ltd. while following up airborne EM anomalies (Golder Assoc., 2010). Later drilling of the Eagle's Nest and Eagle Two deposits by Noront resulted in the discovery of the Blackbird chromite deposits in 2008. In the same year, Freewest discovered the Black Thor deposit while testing a 3.5 km ground gravity anomaly (Freewest, 2009a). In 2009, the Black Label chromite deposit, located 150 m northwest of the Black Thor horizon, was discovered while testing a target in the Black Thor footwall (Freewest, 2009b). Also in 2009, Probe Mines, while drilling gravity and magnetic anomalies, discovered the Black Creek deposit, along strike and southwest of the Black Thor horizon (Palmer, 2010). The most recently discovered chromite deposit, Black Horse (e.g. Aubut, 2015b), was intersected in 2011 during deep drilling, for Ni-Cu-Pt mineralization, by Fancamp Exploration Ltd.

Of the six chromite deposits discovered, three appear to be located at the same stratigraphic position (Black Thor, Black Creek, Big Daddy; Aubut, 2015a). The Black Label chromite body sits stratigraphically below Black Thor. The Black Thor, Black Creek, Big Daddy, Black Horse and Black Label deposits are tabular bodies striking northeast-southwest and variably dipping steeply, northwest (overturned) to steeply southeast. Thicknesses of the chromite layers vary from a few metres to greater than 100 metres and are typically tens of metres. The Blackbird chromite body which is up to 40 m thick, is overturned and dips moderately to the northwest (Golder Assoc., 2010) and comprises multiple, likely fault dismembered lenses. The Black Horse deposit does not appear to have a near-surface expression as it is bounded by a moderately, northwest dipping shear zone, likely the same one forming the northern margin of the chromite mineralized intrusion at Blackbird (DEIC). All of the chromite bodies were originally stratiform and are hosted by an ultramafic dominated sill complex comprising dunite, peridotite, pyroxenite and gabbro and their serpentinized or talc-carbonate altered equivalents (Mungall et al. 2010, Carson et al. 2015, Houlé et al. 2017). The relative sizes of the deposits are shown in Table 1.

Table 1: Resource estimates, Ring of Fire chromite deposits, 20% Cr_2o_3 cut-off for all deposits except Blackbird, 30% Cr_2o_3 cut-off.

Deposit	Classification	Tonnes (millions)	Grade (%Cr_2O_3)
Black Thor[1]	Meas. & ind.	137.7	32.2
	Inferred	26.8	29.3
Black Label[1]	Meas. & ind.	5.4	25.3
	Inferred	0.9	22.8
Big Daddy[1]	Meas. & ind.	29.1	31.7
	Inferred	3.4	28.1
Black Creek[2]	Meas. & ind.	8.6	38.0
	Inferred	1.6	37.8
Blackbird[3]	Meas. & ind.	20.5	35.8
	Inferred	23.5	33.1
Black Horse[4]	Inferred	85.9	34.5

1. Aubut, 2015a
2. Murahwi and Spooner, 2015
3. Burgess et al., 2012
4. Aubut, 2015b

In the years immediately following the discoveries, intensive drilling was carried out on the deposits. The amount of drilling has diminished since 2012 and consolidation of the claim groups has reduced ownership of the chromite deposits to two companies and their joint venture partners.

PHYSICAL ROCK PROPERTIES

In order to better understand the geophysical responses from the RoF area, it is instructive to look at the physical rock property data. A considerable number of magnetic susceptibility and specific gravity measurements have been obtained from drill core and outcrop by the Ontario Geological Survey (OGS). There is only limited electrical resistivity information available from the area.

Magnetic Susceptibility

Figure 4 shows the compiled magnetic susceptibility data from over 1,000 core and outcrop measurements. The magnetic susceptibilities have been composited into 14 of the rock units used in the regional geological compilation (Metsaranta et al., 2017). It is quite evident from the data that there is a large spread of magnetic susceptibilities, ranging from about 0.024 to 836 x10^{-6} SI. As the ranges of magnetic susceptibilities within rock types are large, there is considerable overlap between rock types and, with the possible exception of iron formation (included in the chemical metasediments designation), it is not possible to deduce rock type from magnetic susceptibility. As we will see later, interpretation of aeromagnetic data alone can be misleading.

In spite of this, and with a couple of exceptions, magnetic susceptibilities are generally lower for the more felsic rocks (near the top of Figure 4) and increase for progressively more mafic rocks. Note that the hornblende magnetite granodiorite unit, despite its felsic composition, has a median magnetic susceptibility that is considerably higher than the mafic rocks and is similar to the ultramafic units (peridotite, pyroxenite and dunite). Also, the oxide-poor Neoarchean mafic intrusive rocks (gabbro), inferred to be comagmatic with the chromite mineralized ultramafic rocks, have generally low magnetic susceptibilities that are similar to those units with a more felsic composition. As would be expected (e.g. Ali and Khan, 2013), chromitite has low magnetic susceptibility.

Specific Gravity

The specific gravity (SG) data, compiled from 861 hand samples, is shown in Figure 5. Granodiorite, the most felsic of the rocks, has low SG's with a median value of 2.68 g/cm^3. Densities of the different rock types generally increase as the composition becomes progressively more mafic, which is to be expected. However, the ultramafic rocks (peridotite, pyroxenite and dunite), which host the chromite mineralization, are much less dense than would be anticipated (e.g. Parasnis, 1971, Telford et al., 1990). Dunite samples yielded a median SG of 2.63 g/cm^3, less even than granodiorite. The anomalously low densities appear to be due to serpentinization or talc-carbonate alteration of the ultramafic rocks. Chromitite, on the other hand, is distinguished by values greater than 4.1 g/cm^3 and a median value of 3.8 g/cm^3 which suggest that gravity should be a suitable exploration tool.

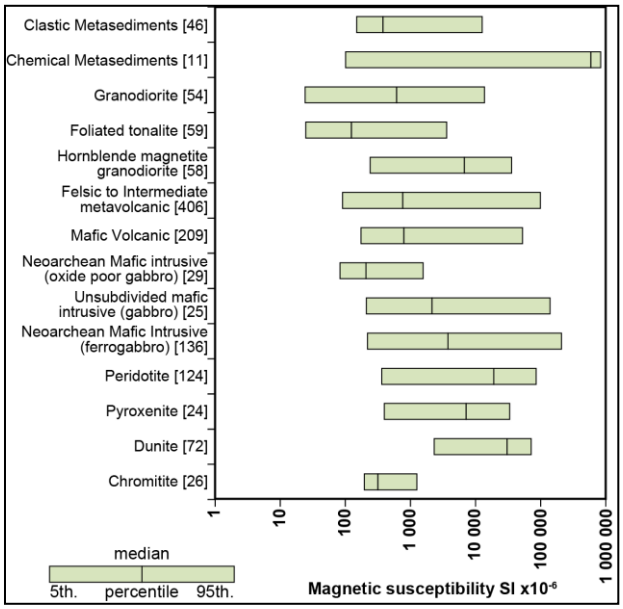

Figure 4: Compiled magnetic susceptibility results of principal rock types from the RoF. The number of samples measured, for each rock type is shown in square brackets.

Note that the amount of overlap of density ranges between units is much less than for magnetic susceptibility and does, therefore, make it a better predictor of rock type. This is frequently the case as density is controlled by the bulk chemistry of a rock, whereas magnetic susceptibility is largely an expression of concentration of magnetite which is most often merely an accessory mineral.

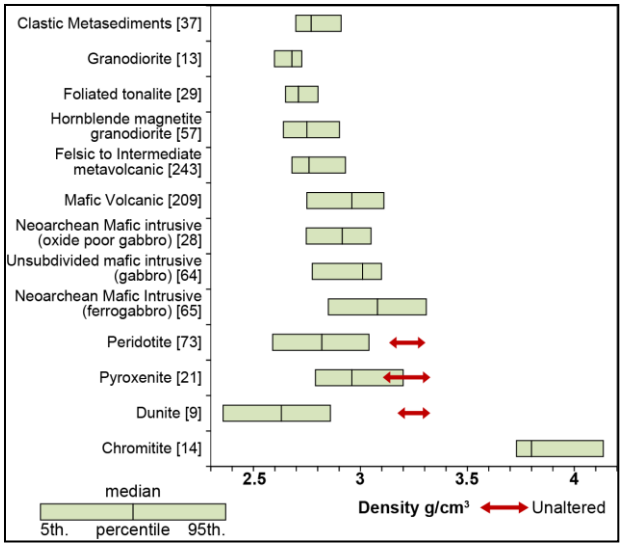

Figure 5: Compiled SG results of principal rock types from the RoF. The number of samples measured for each rock type is shown in square brackets. Unaltered ranges from Parasnis (1971).

Electrical Properties

Although electrical rock property data from the RoF region are sparse, there is evidence that the ultramafic rocks which host the chromitite mineralization are relatively conductive. Correlations between ultramafic rocks and conductive responses have been observed in the results of airborne and ground EM surveys. Similar associations have been observed in other parts of the world (e.g. Palacky, 1988).

The results (Figure 6) of a downhole induced polarization (IP)/resistivity survey (JVX, 2009), from a hole drilled along the main trend of the chromite mineralization, show a dramatic decrease in apparent resistivity from over 1,000 ohm-m in adjacent granodiorite to less than 1 ohm-m within the peridotite unit. The effect of serpentinization on the resistivity of ultramafic rocks has previously been documented by Frasheri et al. (1995) and it is likely to account for the low values of the peridotites along with the possible effects of paleo-weathering.

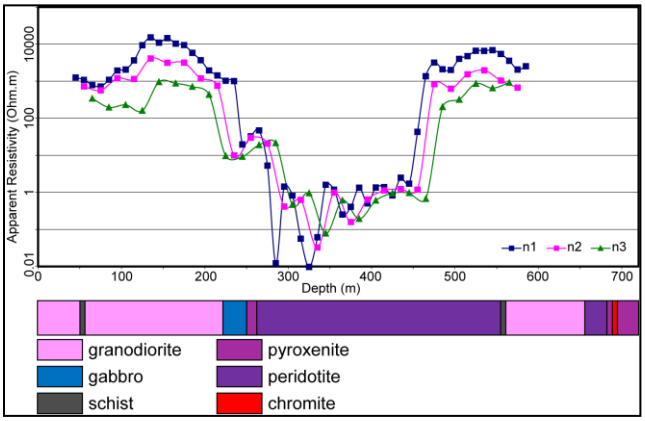

Figure 6: Downhole pole-dipole apparent resistivity profiles (a=20m, n=1,2,3) from drill hole NOT-08-40 (after JVX, 2009) with lithologies simplified from drill log (courtesy Noront Resources Ltd.).

MAGNETIC AND GRAVITY RESPONSES

Once the significance of the initial chromite discoveries had been appreciated, attention turned to the use of magnetic and gravity methods to help define the mineralized horizons. As we have seen from the physical rock properties, the ultramafic rocks that host the chromite deposits have generally higher magnetic susceptibilities and lower densities than the surrounding country rock. The chromite mineralization itself is considerably denser than the host rocks, but has very low magnetic susceptibility.

The ground magnetic and gravity responses over the Big Daddy and southwest end of the Black Thor and Black Creek deposits (Figures 7a and 8a) are typical of those obtained over the near-surface tabular chromite horizons (i.e. excluding the Blackbird and Black Horse deposits). A well-developed high magnetic region (Figure 7a), with an amplitude of approximately 7,000 nT, is centred on the northwest flank (footwall) of the mineralization. Extensive drilling of the deposits has shown that the magnetic features correspond to the serpentinized ultramafic rocks that host the chromite horizons. An approximately 500 m offset in the magnetic response between the Big Daddy and Black Thor deposits suggests that Big Daddy is the faulted extension of Black Thor.

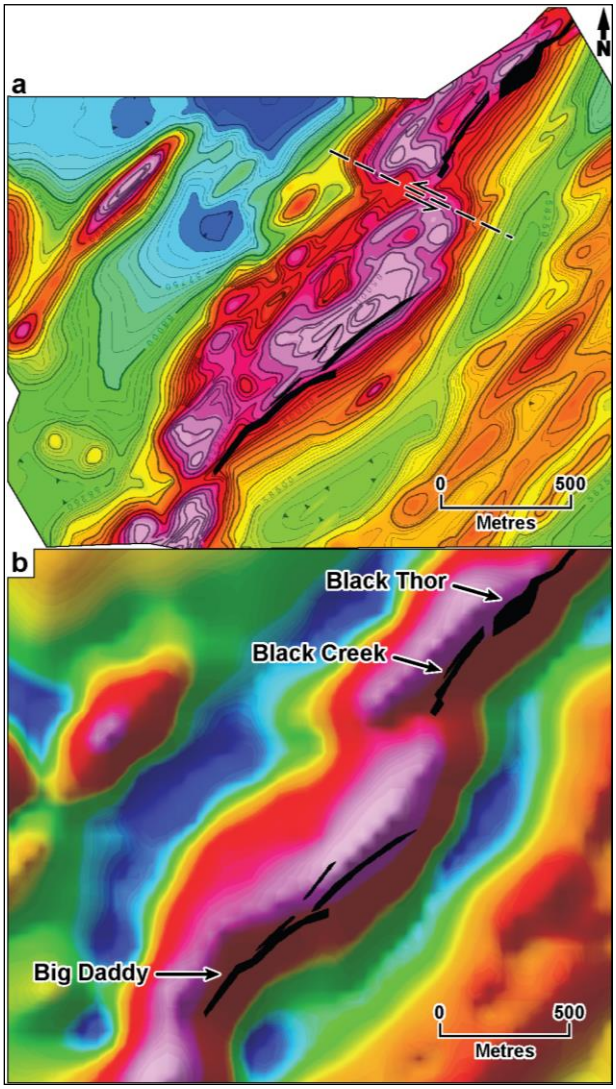

Figure 7: Ground and airborne magnetic images over the Big Daddy and the southwest part of the Black Thor deposit. Black polygons show the surface projection of mineralization. a) Ground total magnetic field (courtesy KWG Resources Inc. and Noront Resources Ltd..), data range approximately 6700 nT; b) Airborne first vertical derivative of the residual magnetic field (data range 24 nT/m).

The residual Bouguer anomaly data from the ground gravity data (Figure 8a) shows linear highs, with an amplitude of 0.6 mGal strongly correlated with the chromite horizons. The broad widths of the mineralization along with the high density of the chromite and its proximity to surface combine to create a very well-defined gravity anomaly. The broad gravity low, parallel with and northwest of the Big Daddy deposit, is almost certainly due to the anomalously low density of the ultramafic host rocks that lie mostly in the footwall.

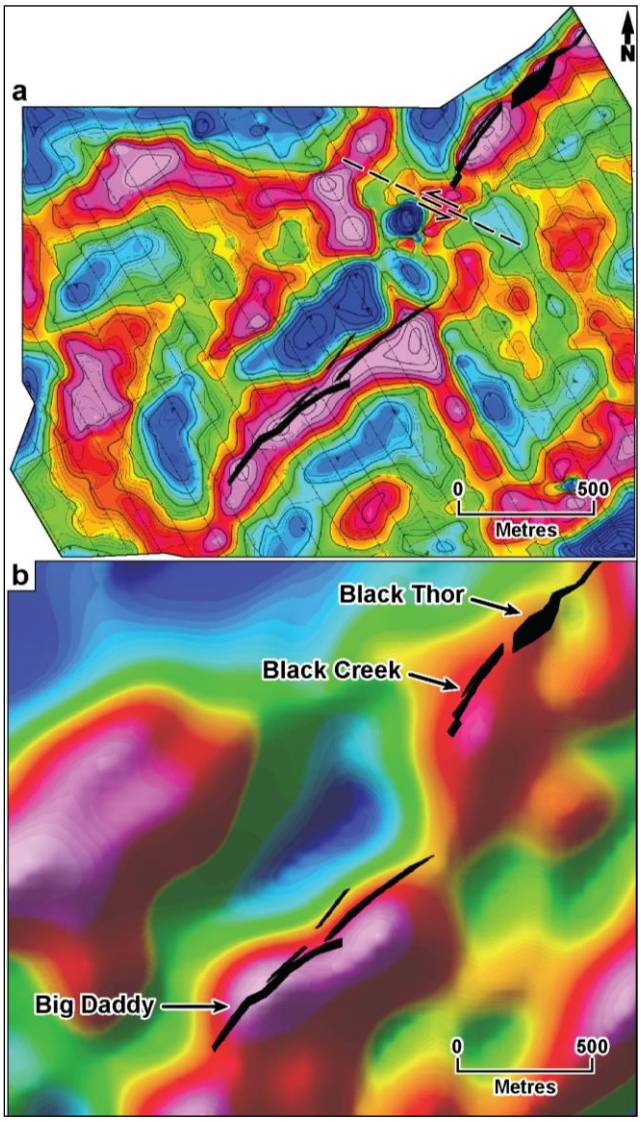

Figure 8: Ground and airborne gravity images over the Big Daddy and southwest part of the Black Thor deposit. Black polygons show the surface projection of mineralization. a) Residual Bouguer ground gravity anomaly (500 m high pass filtered, data range 1 mGal), data courtesy KWG Resources Inc. and Noront Resources Ltd.; b) Airborne vertical gravity gradient (data range 100 Eötvös).

The airborne magnetic and gravity gradiometer responses from a Falcon survey (Ontario Geological Survey and Geological Survey of Canada, 2011) jointly commissioned by the OGS and the Geological Survey of Canada (GSC) are shown in Figures 7b and 8b. Although lacking the resolution of the ground magnetic survey, the first vertical derivative of the aeromagnetic data clearly shows the magnetic response of the ultramafic rocks on the northwest side of the mineralized trend.

The airborne vertical gravity gradient, unlike the ground data, does not unambiguously outline the chromite horizons. Instead, it defines a 2 km wide, northeast striking zone of high gradient values that corresponds to the broader package of mafic intrusive rocks (oxide-poor gabbro and ferrogabbro) and mafic to felsic metavolcanic rocks . Forward modelling (Rainsford, 2013) using typical deposit geometry and densities of the chromite and adjacent rocks confirmed that, while the airborne gravity data are capable mapping of mapping major geological units, there was insufficient signal from the mineralization itself to be able to resolve it above the background noise (survey and geological).

Smooth model inversion (using UBC-GIF software, Oldenburg et al., 1998) of the airborne magnetic and gravity data (Figures 9a and 9b) recovers a steeply dipping magnetic body abutting the northwest flank of the chromite horizon and broader, high-density body along the southeast side. The magnetic and gravity models correspond closely to the known extents of the ultramafic host rocks and the McFaulds Lake mafic rocks respectively.

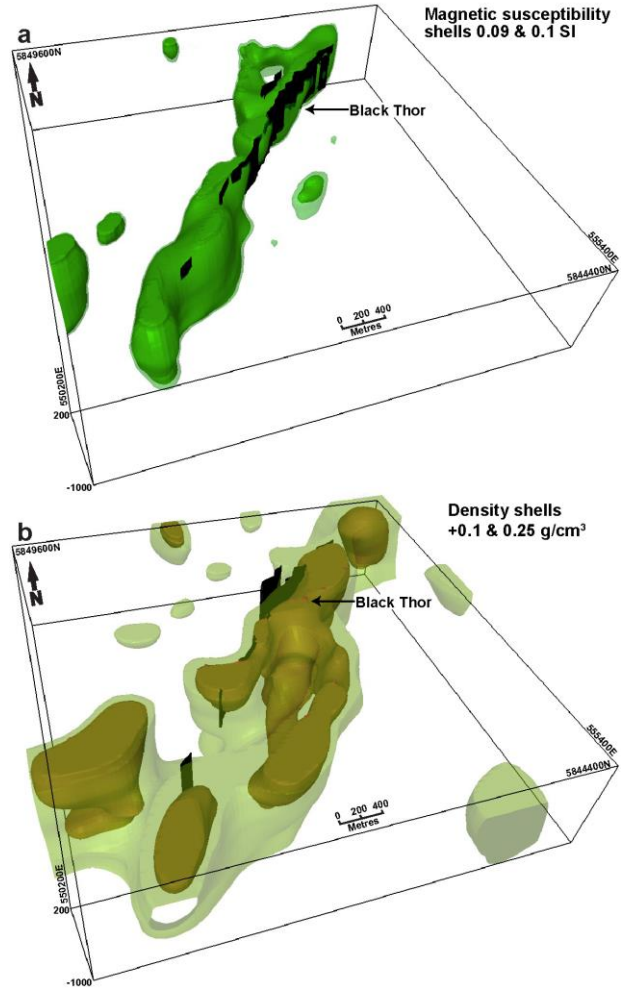

Figure 9: a) Smooth model magnetic inversion showing 0.1 and 0.09 SI magnetic susceptibility isosurfaces, b) Smooth model gravity inversion showing +0.1 and +0.25 g/cm^3 density contrast isosurfaces. Black solids show chromite mineralization. Data from airborne gravity gradiometer and magnetometer survey

(Ontario Geological Survey and Geological Survey of Canada, 2011).

ELECTROMAGNETIC RESPONSES

As has been noted in our discussion of the chromite discovery history, it was the targeting of EM anomalies in the search for massive sulphide mineralization that led to the initial discovery of chromite in the RoF district. The horizontal loop EM (HLEM) response from the ground survey used to follow-up of airborne GEOTEM anomalies is shown along with the results of the discovery hole in Figure 10.

There is a strong correlation between the position of the EM and magnetic responses with the location of the ultramafic sills that host the chromite mineralization. The HLEM profiles suggest a narrow conductor, however as no sulphides were observed in the core, it is probable that the EM anomaly is caused by the altered (serpentinized) ultramafic rocks recorded on the drill log.

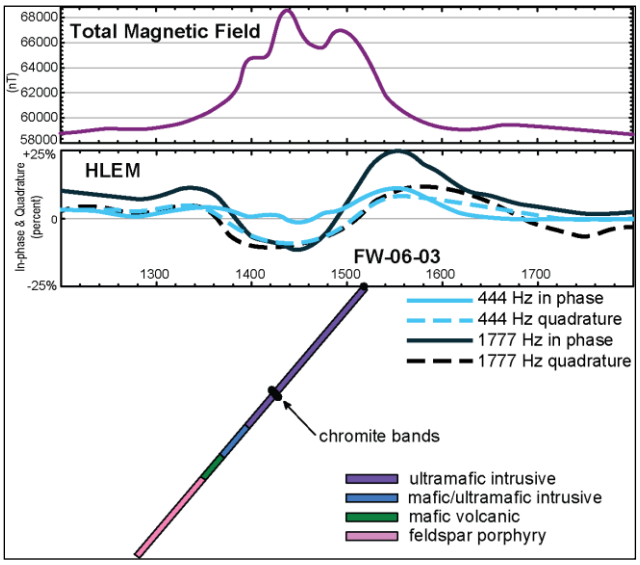

Figure 10: Ground magnetic and HLEM profiles used to target conductivity anomaly the led to the intersection of chromite bands in drill hole. Coil separation is 100 m. HLEM data courtesy KWG Resources Inc.

Subsequent to the initial GEOTEM survey, several other airborne EM systems have been flown in the RoF including, AeroTEM, VTEM and Z-TEM. The use of these systems in the RoF has been reviewed in some detail by Balch et al., (2010). All of these airborne EM systems were able to define conductive responses, closely associated with the chromite mineralized trend, that are now largely understood to be caused by the conductivity of the altered ultramafic host rocks. Figure 11 illustrates the EM conductance defined by an AeroTEM system over the Black Thor and Big Daddy deposits.

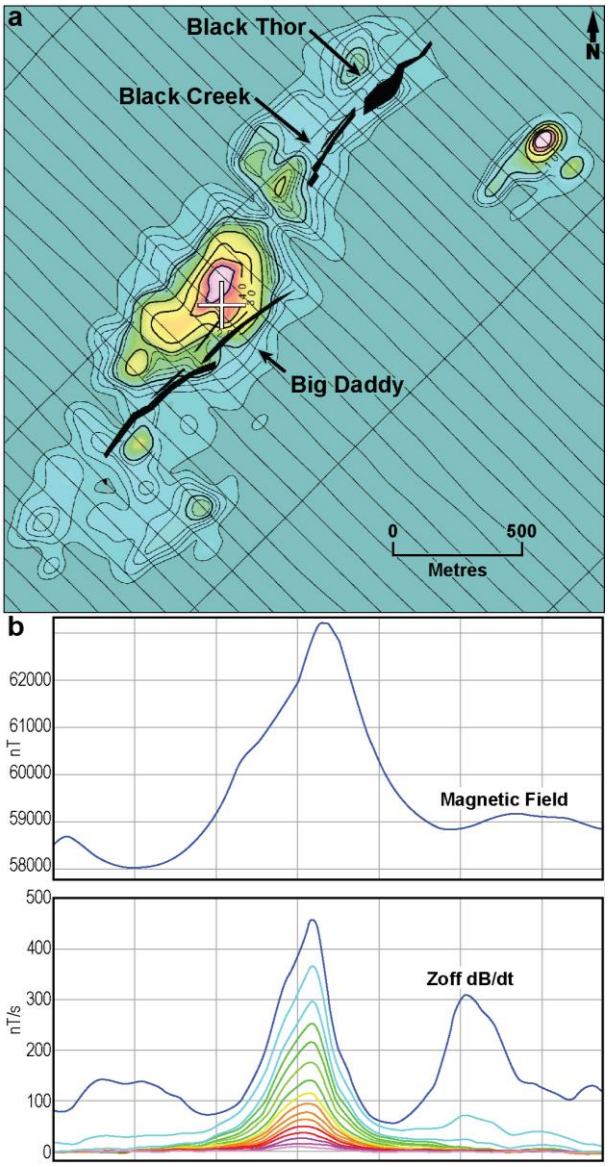

Figure 11: a) AeroTEM apparent conductance image over the Big Daddy and Black Thor deposits, (EM conductance range 60 S); b) typical EM decay responses (note position of cursor in top panel). Data courtesy KWG Resources Inc. and Noront Resources Ltd.

GEOPHYSICS USED TO UPDATE THE GEOLOGICAL INTERPRETATION

An important part of the chromite story is the improvement in the geological understanding of the area. Owing to the remoteness of the region and lack of outcrop, the geology of the RoF was poorly understood and had received relatively little attention. The James Bay lowlands had first been explored along the Albany and Attawapiskat Rivers by Robert Bell in 1885 (Bell, 1886). The GSC published the first geological map in 1962 (Bostock, 1962), which was followed by further mapping and compilation by the OGS (Thurston et al., 1972). A compilation of the Hudson Bay and James Bay lowlands area,

drawing heavily on aeromagnetic data, was published in 2008 (Stott, 2008). The latest geological mapping and compilation, making use of recent exploration drill results and modern geophysical surveys, was published this year (Metsaranta and Houlé, 2017a, b, c).

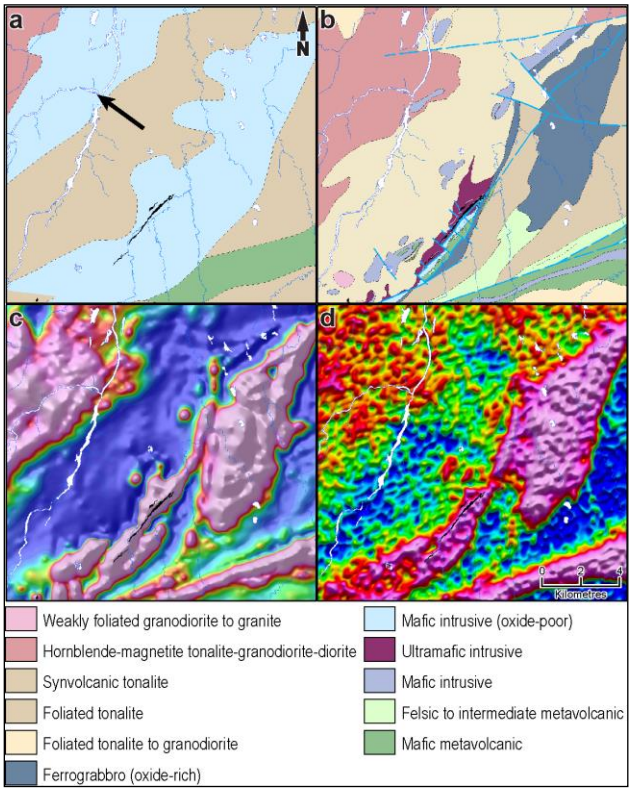

Figure 12: Example of ability of airborne gravity to improve understanding of geology. a) Previous geological map largely interpreted using aeromagnetic data (after Stott, 2008), b) Recently published geology map (after Metsaranta and Houlé, 2017b); c) total magnetic field (data range 6,200 nT); d) vertical gravity gradient (data range 160 mGal/m). Note location of chromite mineralization in black.

The improvement in the most recent geological map over the previous version is illustrated in Figure 12. Figure 12a shows an excerpt of the geology from the 500,000 scale, 2008 compilation adjacent to the 100,000 scale geological map published in 2017 (Figure 12b). Unsurprisingly, Figure 12b shows a much higher level of detail than the earlier map, bearing in mind the difference of map scale and the additional information that was available for the compilation of the later map. Setting aside the differences in scale and data density, we see that Figure 12a shows a large mafic intrusive unit in the northwest corner (highlighted with an arrow) which is not present in the updated geological map (Figure 12b). When we look at the magnetic image (Figure 12c), it is apparent that the magnetic data were largely used to infer the presence of the mafic intrusive. However, the airborne vertical gravity gradient image (Figure 12d) shows no evidence of a high density body that would be expected to be associated with a mafic intrusive body, whereas the mafic and ultramafic rocks along the main chromite horizon and elsewhere are outlined by high gravity gradient responses.

This example, where the magnetic pattern of granitoid rocks mimics those with mafic composition, shows that the interpretation of magnetic data alone can be misleading, especially in areas like the James Bay lowlands where outcrop is very sparse. The mapping of density variations in bedrock with airborne gravity (particularly gravity gradiometry), simply by distinguishing between areas with felsic and mafic compositions, greatly improves the understanding of the geology. From a mineral exploration perspective, airborne gravity combined with regional magnetic data provides a means of rapidly identifying areas of mafic and ultramafic rocks that may be favourable hosts to chromite, massive sulphide (volcanogenic or magmatic), titanium-vanadium and precious metal mineralization. In the particular case of the RoF region, it is possible to reduce the area of interest to about 20% of the whole and thus focus exploration efforts more effectively. However, given the observed density loss related to hydration (serpentinization and/or talc-carbonate alteration) of ultramafic rock units in the RoF, gravity data may not fully express the distribution of ultramafic intrusive rocks.

REGIONAL GEOPHYSICAL MODELLING, CLASSIFICATION AND INTERPRETATION

3D inversion of potential field data has been widely accessible to the exploration community since the mid-1990s. Data compression and parallel computing now allow inversion of large surveys at low cost. With multiple voxel models of considerable size, in this case density and susceptibility, it is inherently difficult to visualize, assimilate and interpret the results. One approach, of course, is to simply subset or slice and section the voxel models and use these in a conventional manner in GIS or other environments. Alternatively, one can create isosurfaces (3D contours) and simultaneously display apparent density and susceptibility information in three dimensions along with available drill hole and surface geology. The sheer size of the regional 3D models limits the practicality of either approach when attempting to combine and interpret multiple parameters at the same time.

A simple but effective imaging approach is illustrated in Figure 13. Here the density and susceptibility models have been sliced 100 m below the topographic surface and are compared to the recently released geologic map by Metsaranta and Houlé (2017b). Since many features of this map were defined using magnetic and gravity data it is not surprising that many of the main lithologic features are readily recognizable on the combined image. There are however, a number of features which are only recognizable on the combined image.

Multiparameter Classification of 3D models

Alternatively, conventional clustering and classification schemes can be used to combine multiple parameters into a single representation of both dataset. *Clustering* is the task of grouping a set of objects so that objects in the same population (cluster) are more similar to each other in some sense than to those in other populations. It is unsupervised. For example: sort emails

into groups by content. *Classification* is the task of assigning an object to one of a set of predefined populations (classes). It is supervised, for example: sort emails into two classes namely, spam | not spam based a user-defined rule.

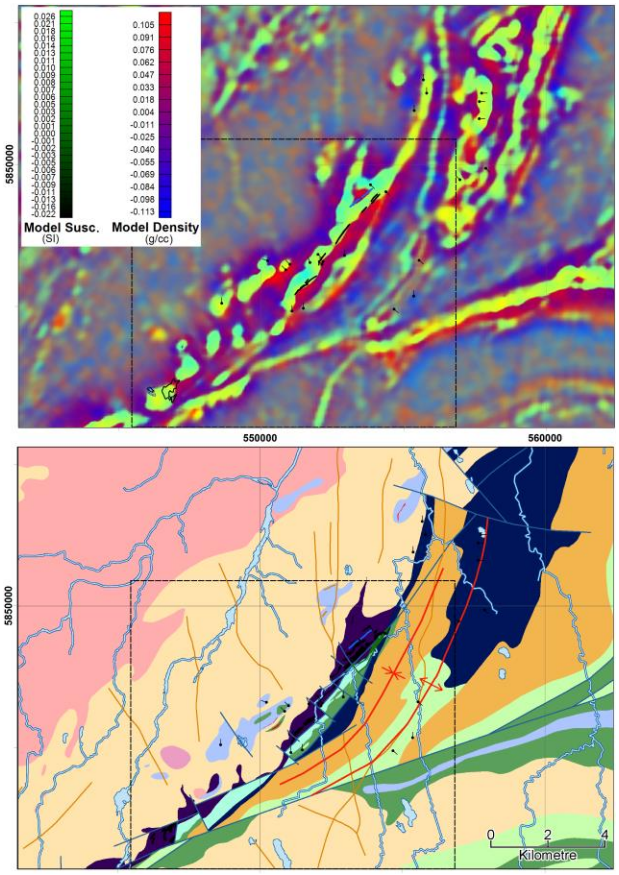

Figure 13: Combined density and susceptibility depth slice image (upper) and corresponding geology map modified from from Metsaranta and Houlé (2017b), Houlé et al. 2017 (lower). Geology legend is the same as Figure 1.

Examples of clustering were presented in Oldenburg and Pratt (2007) and Fraser (2013). In both cases they rely on an algorithm to identify natural groupings in the data and then present these groups as 3D models.

However, examination of a simple scatterplot of model density versus susceptibility (Figure 14) shows that identifying meaningful, natural clusters is challenging and here we deploy an alternative approach where the user can control and manipulate the class boundaries.

Modelling Considerations

It is well known that models produced by inversion of potential field data are non-unique and depend on many parameters in addition to the data namely: the error assigned to each measurement, the regularization (e.g. smoothness, depth weighting etc.), model parameterization, external constraints and details of the inversion algorithm. Since one objective is to combine 3D density and 3D susceptibility models into a single model we deliberately attempt, whenever possible, to keep aspects of the inversion identical for both datasets. The magnetic field and gravity gradient data were collected simultaneously from the same platform so the system geometry is identical. Gravity gradient and magnetic field data are linearly related through Laplace's equation so we can use identical inversion algorithms. Although it is natural to use identical model parameterization (e.g. voxel dimension) and identical regularization, the signal to noise ratio is much lower for airborne gravity gradient data compared to total field magnetic data and this must be considered during model construction. Since data misfit strongly affects the smoothness and variance of the resulting model we choose to assign higher than necessary error to the magnetic data to produce a susceptibility model which matches the characteristics of the density model.

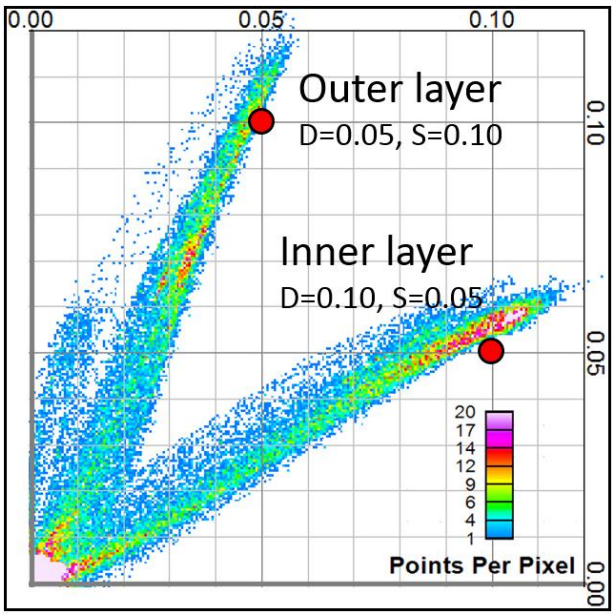

Figure 14: Cross-plot of density vs. susceptibility from the synthetic fold model shown in Figure 15. In this case both models were constrained to allow only positive physical properties.

Inversion of Synthetic Data

Synthetic datasets created by forward modelling the response from simple, known geometries are used to shed light on our ability to recover density and susceptibility and provide insight into approaches for assigning class boundaries. The process is illustrated diagrammatically in Figure 15 and a cross-plot of density vs. susceptibility is shown in Figure 14. This shows that rather than forming a cloud of points centred on the known physical parameters which were used to create the input data(red circles), the inversion has smeared the result into streaks radiating from the origin and this suggests the form that "radial" class boundaries may be useful when classifying the 3D models as illustrated in Figure 16.

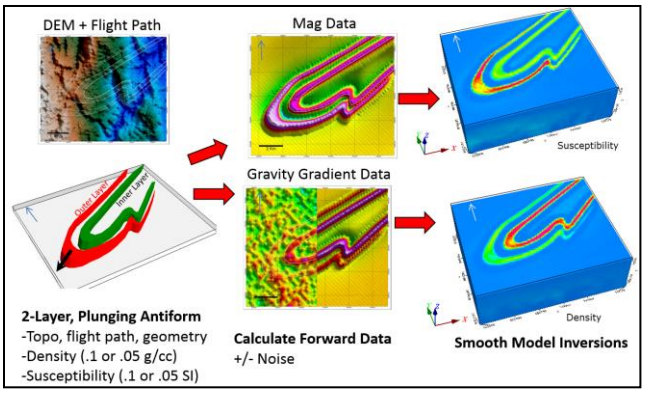

Figure 15: Schematic showing simulated data and models used to establish classification criteria.

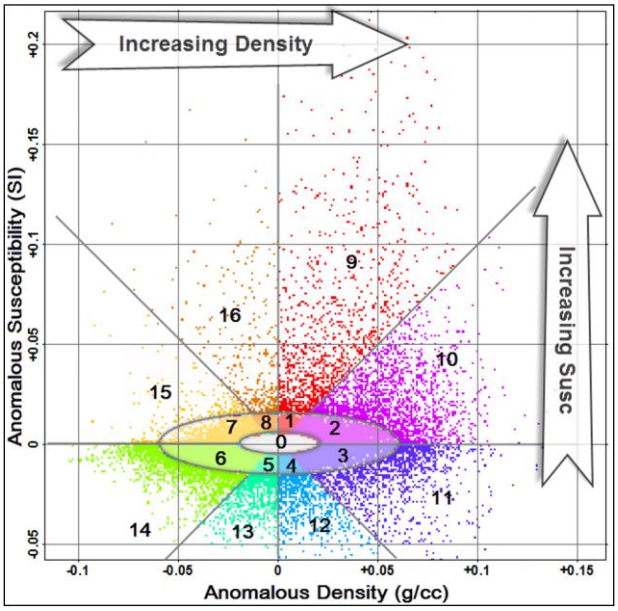

Figure 16: Classifications assigned to density and susceptibility to produce the map shown in Figure 18.

Classification of 3D models

In this example we assign arbitrary, radial boundaries at 45^{o} intervals to a slice of data from the McFaulds Lake 3D density and susceptibility models (Figure 17). Adjacent classes are assigned similar colours and brighter shades are assigned to the more anomalous classes.

The following observations are made about the classified model shown in Figure 18:

1. Modest density, highly magnetic class [9] forms the footwall to the deposits. This is interpreted to be dunite with its density depressed and magnetite content increased by serpentinization.
2. Dense but relatively weakly magnetic mafic intrusive rocks (class [11]), pyroxenite or ferrogabbro, are interpreted to form the stratigraphic hanging wall.
3. The Chromite deposits are closely mapped into a narrow zone of class [10] (peridotite + chromite) at the contact between classes [9] and [11].
4. Low density plus high susceptibility class [16] is inferred to reflect the highly altered basal part of the intrusions. This class is globally rare and it is also associated with the Eagles Nest Ni-Cu sulphide deposit.
5. Low susceptibility and moderate density class [12] maps the gabbroic upper part of the intrusions and mafic volcanics.
6. Felsic/intermediate volcanic and intrusive rocks are inferred to dominate relatively low density and low susceptibility classes [13] and [14].

This illustrates that, despite the simplicity and arbitrary nature of the classification scheme, a surprising amount of geologically meaningful information can be extracted.

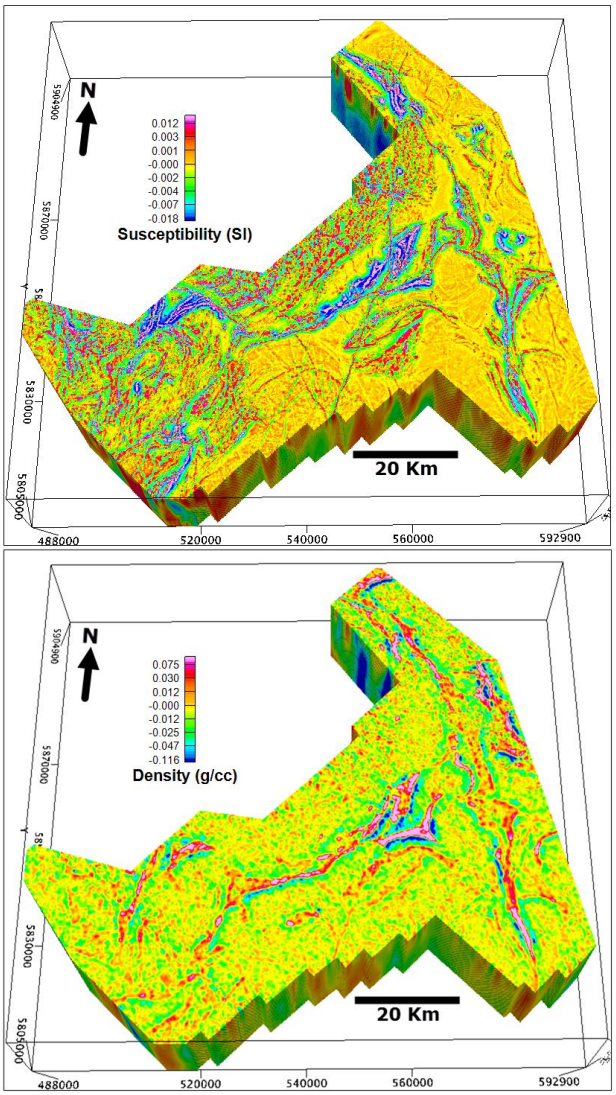

Figure 17: 3D models of density (lower) and magnetic susceptibility (upper).

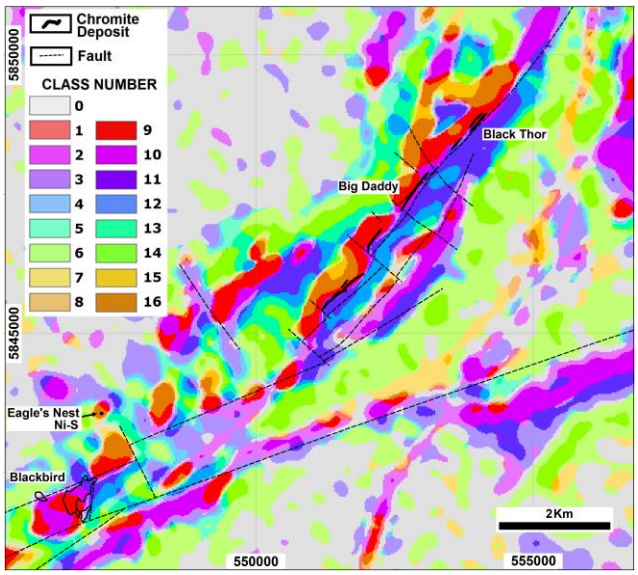

Figure 18: Classified representation of the central McFaulds Lake density and susceptibility data. Faults are shown for visual reference only and are taken from Metsaranta and Houlé (2017b). See dashed rectangle, Figure 13, for location of this figure.

FUTURE DIRECTIONS

All the chromite discoveries made to date, with the exception of the Black Horse deposit, have been near-surface (subcropping). Four of the six discoveries (Black Thor, Black Label, Big Daddy, Black Creek) were detectable using ground gravity; magnetic data served to outline the ultramafic footwall rocks. At least three, nearby, ultramafic-mafic intrusions, Wi, Big Mac, Ley Lake (Figure 1) have similar ages or geological characteristics to the intrusions hosting the main occurrences of chromite and Ni-Cu-PGE mineralization in the RoF (Metsaranta and Houlé, 2017a, b, c). These remain relatively unexplored and still have potential for near-surface mineralization that could be detectable using the same techniques that led to the existing discoveries.

As two of the known chromite deposits, which have no attributable gravity response due to structural dismemberment (Blackbird) or depth (Black Horse), have demonstrated there is still potential to find blind deposits. To do this, attention will need to be directed towards delineating favourable host stratigraphy. The serpentinized ultramafic sills that host the chromite mineralization have been shown to be moderately to weakly conductive and traceable using airborne and ground EM. In order to image the host rocks at depth, deep penetrating EM techniques, such as TDEM, AMT and CSAMT along with IP/resistivity and hybrid IP/AMT methods, are expected to be effective. These methods are unlikely to be able to identify chromite mineralization directly and additional information such as lithogeochemical indicators may be required to vector towards mineralization.

As the depth to targets increases we also expect to see increased used of borehole detection methods notably borehole gravity, magnetics and EM.

In view of the scarcity of outcrop in the region, the geology away from the central part of the RoF is still poorly known. Inversion modelling of the airborne magnetic and gravity data, followed by classification of the results, has shown some promise in predicting the geology. The introduction of a third parameter, such as EM conductivity, could be used to refine this approach further. With regards to exploration, better characterization of the geology furthers the goal of minimizing risk by reducing the size of the target area.

CONCLUSIONS

The RoF represents an increasingly rare example of a new, polymetallic camp being discovered in virgin territory within recent times – one in which modern exploration methods were brought to bear. The history of chromite exploration in the RoF has shown how the recognition of the significance of a narrow intersection, discovered by chance while drilling for a different deposit type, could, within a six-year period, lead to the delineation of six world-class chromite ore bodies. This has been made possible by the rapid evaluation of the geophysical responses associated with the chromite mineralization and adapting the geophysical programs to capitalize on the physical properties of the deposits and their host rocks. Although the time to identify a major new mining district in such a remote area with hardly any outcrop was remarkably short, a burst of activity by many exploration companies and contractors, involving a host of geoscientists, technicians, drillers and others, was required to achieve this.

As we have seen the physical properties of the chromite mineralization and host rocks have made it quite amenable to exploration by geophysical methods, especially as most of the deposits, so far discovered, are near-surface, wide and laterally continuous. As the camp matures, it is to be expected that the "low hanging fruit" will have been found and the challenge will be to find deeper deposits. The Blackbird and Black Horse deposits are already two cases that are essentially blind and are not detectable using the same magnetic, gravity and EM methods used to define the four other known deposits. It is likely that the location of deeper deposits will require the tighter integration of 3D geological information with deep-penetrating geophysical methods designed to detect responses from favourable host stratigraphy rather than the mineralization itself. Also, lithogeochemical markers will be important for identifying fertile host rocks and vectoring towards mineralization. Despite extensive exploration in the central RoF region, additional ultramafic-mafic intrusions, known to be time-correlative with the main occurrences of chromite and Ni-Cu-PGE mineralization in the RoF, have not seen application of the ground geophysical exploration methods that appear to be required to effectively delineate chromite targets. As such, opportunities still exist for additional near-surface discoveries.

We should not forget that reconnaissance-scale stream sediment sampling had identified highly anomalous chromite samples from the Attawapiskat River, 40 km south-southeast of the main

chromite trend. These samples were collected in 1996 by KWG Resources Inc. in 1996 and the results were published (Crabtree and Gleeson, 2003), three years before the first chromite was discovered in bedrock; reminding us again of the importance of integrating all geoscience data. The history of the RoF is still young; the first chapter of which has barely been written.

REFERENCES

Ali, M. and M.J. Khan, 2013, Geophysical Hunt for Chromite in Ophiolite: Int. J. Econ. Environ. Geol.,4 (2), 22-28.

Armstrong, D.K., 2011, Re-evaluating the hydrocarbon resource potential of the Hudson Platform: Interim results from northern Ontario: Summary of Field Work and Other Activities 2011, Ontario Geological Survey, Open File Report 6270, 27-1–27-11.

Aubut, A., 2015a, Black Thor, Black Label and Big Daddy chromite deposits Mcfaulds Lake Area, Ontario, Canada Mineral Resource Estimation Technical Report: NI 43-101 technical report prepared for Noront Resources Ltd.

Aubut, A., 2015b, Koper Lake Project chromite deposits Mcfaulds Lake Area, Ontario, Canada Updated Mineral Resource Estimation Technical Report: NI 43-101 technical report prepared for KWG Resources Inc. and Fancamp Exploration Ltd.

Balch, S.J., J.E. Mungall, and J. Niemi, 2010, Present and Future Geophysical Methods for Ni-Cu-PGE Exploration: Lessons from McFaulds Lake, Northern Ontario: Society of Economic Geologists, Special Publication 15, 559-572.

Bell, R., 1886, Report on an Exploration of Portions of the Attawapiskat and Albany Rivers, Lonley Lake to James Bay: Geological Survey of Canada, Annual Report, Vol 2, 19G.

Bostock H. H., 1962, Geology Lansdowne House Ontario: Map 4-1962, Scale One Inch to Four Miles =1:253,440.

Burgess, H., R. Gowans, C. Jacobs, C. Murahwi, and D. Bogdan, 2012, NI 43-101 technical report feasibility study Mcfaulds Lake property Eagle's Nest project James Bay lowlands Ontario, Canada: for Noront Resources Ltd.

Carson, H.J.E., C.M. Lesher, and M.G. Houlé, 2015, Geochemistry and petrogenesis of the Black Thor intrusive complex and associated chromite mineralization, McFaulds Lake greenstone belt, Ontario, in D.E. Ames and M.G. Houlé eds., Targeted Geoscience Initiative 4: Canadian Nickel-Copper-Platinum Group Elements-Chromium Ore Systems — Fertility, Pathfinders, New and Revised Models, Geological Survey of Canada, Open File 7856, 87–102.

Crabtree, D.C. and C.F. Gleeson, 2003, Results of the "Spider 3" regional kimberlite indicator mineral and geochemistry survey carried out in the vicinity of the upper Attawapiskat and Ekwan rivers, northern Ontario: Ontario Geological Survey, Open File Report 6097, 127p.

Frasheri, A., L. Lubonja, and P. Alikaj, 1995, On the application of geophysics in the exploration of copper and chrome ores in Albania: Geophysical Prospecting, 43, 743-757.

Fraser, S., 2013, Knowledge from Data Using Self Organizing Maps: Presented at 9th Fennoscandian Exploration and and Mining.

Freewest Resources Canada Inc., 2009a, Annual Report 2008, 8-11.

Freewest Resources Canada Inc., 2009b, Freewest discovers new chromite zone on it's 100%-owned Mcfaulds property, James Bay lowlands, Northern Ontario; Company: press release issue 18th. Feb., 2009.

Golder Associates, 2010, Technical report and resource estimate Mcfaulds Lake project James Bay lowlands Ontario, Canada: NI 43-101 technical report for Noront Resources Ltd., 2 p.

Gowans, R. and C. Murahwi, 2009, NI 43-101 technical report on the Big Daddy chromite deposit and associated Ni-Cu-PGE: for Spider Resources Inc., KWG Resources Inc. and Freewest Resources Inc, 21 p.

Hogg, R.L.S. and S. Monro, 2017, The geophysical history of discoveries in the James Bay Lowlands from the Victor kimberlite to the Ring of Fire copper and nickel deposits, in V. Tschirhart and M.D. Thomas, eds., Proceedings of Exploration 17, 663–669.

Houlé, M.G., C.M. Lesher, E.M. Schetselaar, R.T. Metsaranta, and V.J. McNicoll, 2017, Architecture of magmatic conduits in Cr-(PGE)/Ni-Cu-(PGE) ore systems, in N. Rogers ed., Targeted Geoscience Initiative – 2016 Report of Activities, Geological Survey of Canada, Open File 8199, 55-58.

JVX Ltd., 2009, Report on drill hole IP surveys Mcfaulds lake property James Bay lowlands, Northern Ontario, Fancamp exploration Ltd.: Ontario Assessment Report AFRI # 20006147.

Oldenburg, D. W., Y. Li, C.G. Farquharson, P. Kowalczyk, T. Aravanis, A. King, P. Zhang, and A. Watts, 1998, Applications of Geophysical Inversions in Mineral Exploration Problems: The Leading Edge, 17, 461 - 465.

Oldenburg, D.W. and D.A. Pratt, 2007, Geophysical Inversion for Mineral Exploration: a Decade of Progress in Theory and Practice, in B. Milkereit ed., Proceedings of Exploration 07.

Ontario Geological Survey and Geological Survey of Canada, 2011, Ontario airborne geophysical surveys, gravity gradiometer and magnetic data, grid and profile data (ASCII and Geosoft® formats) and vector data, McFaulds Lake Area: Ontario Geological Survey, Geophysical Data Set 1068.

Metsaranta, R.T., M.G. Houlé, V.J. McNicoll, and S.L. Kamo, 2015, Revised geological framework for the McFaulds Lake greenstone belt, Ontario, in D.E. Ames and M.G. Houlé eds., Targeted Geoscience Initiative 4: Canadian Nickel-Copper-Platinum Group Elements-Chromium Ore Systems — Fertility,

Pathfinders, New and Revised Models, Geological Survey of Canada, Open File 7856, 61–73.

Metsaranta, R.T. and M.G. Houlé, 2017a, Precambrian geology of the Winiskisis Channel area, "Ring of Fire" region, Ontario—northern sheet: Ontario Geological Survey, Preliminary Map P.3804; Geological Survey of Canada, Open File 8200, scale 1:100 000. doi: 10.4095/299708.

Metsaranta, R.T. and M.G. Houlé, 2017b, Precambrian geology of the McFaulds Lake area, "Ring of Fire" region, Ontario—central sheet: Ontario Geological Survey, Preliminary Map P.3805; Geological Survey of Canada, Open File 8201, scale 1:100 000. doi: 10.4095/299711.

Metsaranta, R.T. and M.G. Houlé, 2017c, Precambrian geology of the Highbank Lake area, "Ring of Fire" region, Ontario—southern sheet: Ontario Geological Survey, Preliminary Map P.3806; Geological Survey of Canada, Open File 8202, scale 1:100 000. doi: 10.4095/299712.

Mungall, J.E., J.D. Harvey, S.J. Balch, B. Azar, J. Atkinson, and M.A. Hamilton, 2010, Eagle's Nest: A magmatic Ni-sulfide deposit in the James Bay Lowlands, Ontario, Canada, in .J. Goldfarb, E.E. Marsh, and T. Monecke eds., The Challenge of Finding New Mineral Resources: Global Metallogeny, Innovative Exploration, and New Discoveries, Volume I: Gold, Silver, and Copper-Molybdenum, Society of Economic Geologists, Special Publication 15, 539–559.

Murahwi, C.Z. and J. Spooner, 2015, Updated technical report on the mineral resource estimate for the Black Creek chrome deposit, Mcfauld's Lake area, James Bay lowlands, Northern Ontario, Canada; NI 43-101 technical report: for Probe Mines Ltd., 65 p.

Palacky, G.J., 1988, Resistivity Characteristics of Geologic Targets, in M. Nabighian ed., Electromagnetic Methods in Applied Geophysics – Theory, Investigations in Geophysics, 3(1), 53-129.

Palmer, D., 2010, Mcfauld's West Project James Bay Lowlands, Ontario, Results of VTEM Airborne Survey and Diamond Drilling Program: Ontario Assessment Report AFRI # 20007016.

Parasnis, D.S., 1971, Physical property guide for rocks and minerals: Geophysical Memo 4/71, ABEM.

Rainsford, D., 2013, Airborne gravity gradiometry in the Ring of Fire: Presented at PDAC 2013.

Ratcliffe, L.M. and D.K. Armstrong, 2013, The Hudson Platform Project: 2013 field work and drill-core correlations, western Moose River Basin: Summary of Field Work and Other Activities 2013, Ontario Geological Survey, Open File Report 6290, 36-1–36-19.

Sage, R.P., 2000, Kimberlites of the Attawapiskat area, James Bay Lowlands, northern Ontario: Ontario Geological Survey, Open File Report 6019, 341 p.

Stott, G. M., 2008, Precambrian geology of the Hudson Bay and James Bay lowlands region interpreted from aeromagnetic data – east sheet: Ontario Geological Survey, Preliminary Map P.3598-Revised, scale 1:500,000.

Stott, G.M. and S.D. Josey, 2009, Proterozoic mafic (diabase) dikes and other post-Archean intrusions of northwestern Ontario, north of latitude 49°30′: Ontario Geological Survey, Preliminary Map P.3606, scale 1:1 000 000.

Telford, W.M., L.P. Geldart, and R.E. Sheriff, 1990 Applied Geophysics, Second Edition: Cambridge University Press.

Thurston, P.C., M.W. Carter, and R.A. Riley, 1972, Fort Hope-Landsdowne House sheet, geological compilation series, Cochrane, Kenora, and Thunder Bay districts: Ontario Department of Mines and Northern Affairs, Map 2237, 1:253 440.

Witherly, K and P. Diorio, 2014, Application of airborne magnetics, EM and gravity to the Ring of Fire intrusive complex, Ontario: 84th Annual International Meeting, SEG, Expanded Abstracts, 1704-1708.